

$J_{eff} = 1/2$ Mott Insulating State in Rh and Ir Fluorides

Turan Birol and Kristjan Haule

Department of Physics and Astronomy, Rutgers University, Piscataway 08854, NJ, USA

(Dated: March 1, 2022)

Discovery of new transition metal compounds with large spin orbit coupling (SOC) coexisting with strong electron-electron correlation among the d electrons is essential for understanding the physics that emerges from the interplay of these two effects. In this study, we predict a novel class of $J_{eff} = 1/2$ Mott insulators in a family of fluoride compounds that are previously synthesized, but not characterized extensively. First principles calculations in the level of all electron Density Functional Theory + Dynamical Mean Field Theory (DFT+DMFT) indicate that these compounds have large Mott gaps and some of them exhibit unprecedented proximity to the ideal, $SU(2)$ symmetric $J_{eff} = 1/2$ limit.

Interest in $5d$ compounds has been blossoming in the recent years in response to the scientific advances and applications in the areas of topological insulators, multiferroics, and thermoelectrics. At the forefront of this activity are the Ir compounds, because of the interesting interplay between itinerancy, the electronic correlations and strong spin-orbit coupling (SOC).¹ This strong coupling between the spin and orbital degrees of freedom gives rise to various interesting phases, such as the exotic spin-liquid phase predicted in honeycomb iridates, or the recently observed Fermi arcs and the spin-orbit induced Mott insulating phase in the perovskite-related Ir-oxides.¹⁻⁴ In these latter systems, the SOC splits the six-fold degenerate Ir t_{2g} states into 4 occupied $J_{eff} = 3/2$ and 2 half-occupied $J_{eff} = 1/2$ states. The bands formed by the $J_{eff} = 1/2$ states are much narrower than the width of the whole t_{2g} manifold in the absence of SOC, and as a result, the system can be easily drawn to a Mott-insulating phase with even a modest amount of correlations on the $5d$ Ir atom.⁵⁻⁸

The most widely studied SOC induced correlated insulator is Sr_2IrO_4 , which is an antiferromagnetic insulator below 240 K.^{3,9} There are numerous studies that involve strain, and pressure on this material; and various related compounds are also extensively studied.¹⁰⁻¹⁶ However, despite being the prototypical system, Sr_2IrO_4 is far from being the ideal $J_{eff} = 1/2$ Mott insulator: the existence of the insulating state above the Neel temperature is due to short range order, which is around 100 lattice constants even 20K above the Neel temperature,¹⁷ hence Sr_2IrO_4 was termed a ‘*marginal Mott insulator*’. This marginal nature of the insulating state was confirmed theoretically, as the first-principles calculations, which neglect short range order, predict bad metallic state in the paramagnetic phase.¹⁸ Also, the crystal structure of Sr_2IrO_4 is far from cubic: it has the tetragonal space-group $I4_1/acd$. The tetragonal symmetry breaks the degeneracy of the t_{2g} orbitals, and thus the $J_{eff} = 1/2$ orbitals mix, moving the system away from the ideal limit where the moments are $SU(2)$ invariant. Since $SU(2)$ symmetric $J_{eff} = 1/2$ insulators are proposed to exhibit superconductivity when doped,¹⁹ it is important to identify new compounds that are true $J_{eff} = 1/2$ Mott insulators with sizeable gaps.

In this study, we predict a novel class of $J_{eff} = 1/2$ Mott insulator compounds that are both very close to the $SU(2)$ limit and have large charge gaps in the paramagnetic state. We achieve this by considering crystal structures that are not commonly studied in the context of correlated electron physics. We focus on a group of already synthesized iridium and rhodium fluoride compounds and use first-principles calculations at the level of fully charge self-consistent DFT+DMFT to show the presence of the $J_{eff} = 1/2$ insulating state in these compounds. We thus expand the search for new $J_{eff} = 1/2$ insulators to the family of fluorides, and for the first time show that the $J_{eff} = 1/2$ state can exist in a rhodium compound.

We begin our search for new $J_{eff} = 1/2$ insulators by the well known observation that lower bandwidth favours the Mott insulating phase. The $Sr_{n+1}V_nO_{3n+1}$ Ruddlesden-Popper (RP) series nicely demonstrates this point:²⁰ The $n = \infty$ $SrVO_3$ is a correlated metal. In this compound, the oxygen octahedra are corner sharing, and the number of nearest neighbour transition metal ions is $z = 6$. With decreasing n , z decreases monotonically from $z = 6$ to $z = 4$ for Sr_2VO_4 ($n = 1$). This leads to a decrease of the bandwidth as n decreases, and as a result there is a metal-insulator transition as a function of n , and Sr_2VO_4 is a Mott insulator.²⁰ The $Sr_{n+1}Ir_nO_{3n+1}$ compounds also behave similarly: The perovskite $SrIrO_3$ ($z = 6$) is a correlated metal, the $n = 2$ $Sr_3Ir_2O_7$ ($z = 5$) is barely an insulator, and the $n = 1$ Sr_2IrO_4 ($z = 4$) is the well-known $J_{eff} = 1/2$ insulator.^{3,9}

A strategy to obtain a small bandwidth and hence a possible $J_{eff} = 1/2$ Mott insulator in an iridate compound is to look for crystal structures where the connectivity of anion octahedra is low. The extreme case is a structure that consists of isolated IrO_6 octahedra that are not corner-, edge-, or face-sharing with any other octahedra. But, to the best of our knowledge, there exists no structure with isolated MO_6 units in transition metal oxides. However, isolated hexafluoro-transition metal complexes (MF_6) are known to exist and are very common in fluoride compounds.²¹ The Ir ion in many of these compounds have the d^5 electronic configuration, and hence can lead to the $J_{eff} = 1/2$ Mott insulating

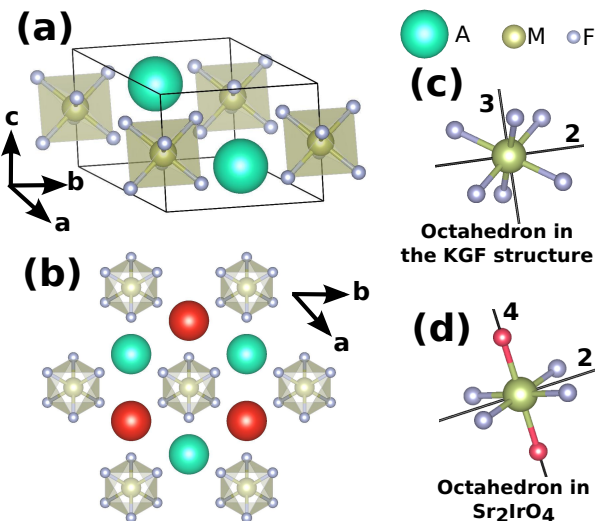


FIG. 1. (a) The K_2GeF_6 (KGF) crystal structure. (b) The MF_6 octahedra are aligned parallel and form triangular layers. The alkali metals are both above and below these layers, shown by green and red. (c) Coordination environment of the transition metals in the KGF and (d) the $n = 1$ RP structure. Chemically inequivalent F ions in the RP structure are shown by blue and red.

phase.

As an example of this group of compounds, we consider the alkali metal hexafluoro-iridates and rhodates with the chemical formula A_2MF_6 and the so called K_2GeF_6 (KGF) crystal structure^{22,23} shown in Fig. 1. Here, A is the alkali metal ion and M is the transition metal ion. Each M ion (in our case either Ir or Rh) is in the center of an F_6 octahedron. The space group is trigonal $P\bar{3}m1$. While there is no symmetry element that imposes the octahedra to be regular, all six M-F bond lengths are equal and the F-M-F angles are close to 90° . The site symmetry of the M ion is $\bar{3}m$, and the threefold degenerate t_{2g} states are split into $2+1$. However, unlike in the RP compound Sr_2IrO_4 , all ligands are symmetry equivalent (Fig. 1c-d), and as a result an equally distorted octahedron is expected to cause a smaller splitting of the t_{2g} states in the A_2MF_6 compounds than in the RP compounds.

The M ions form regular triangular layers (Fig. 1b). The octahedra and the local coordinate axes of all M ions are aligned in a parallel fashion. The out-of-plane lattice constant c is smaller than the in-plane lattice constant a , and as a result, the band structure is of 3-dimensional character. The Ir and Rh cations we consider have $4+$ formal valence and 5 electrons in their t_{2g} orbitals in this structure. Since the MF_6 octahedra are isolated in the sense that there are no F ligands that are coordinated to two different M ions, the effective hopping between the M ions is small and hence the d bands at the Fermi level are expected to be extremely narrow - rendering the system a strong Mott insulator.

In Fig. 2, we show the densities of states

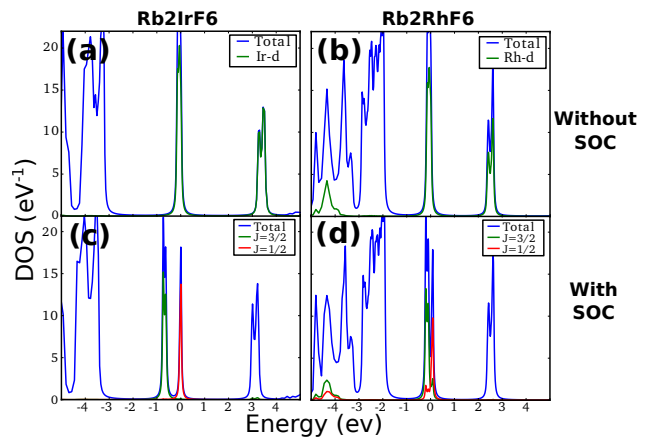


FIG. 2. DOS of Rb_2IrF_6 and Rb_2RhF_6 within Density Functional Theory, with and without spin-orbit coupling.

(DOS) of Rb_2IrF_6 and Rb_2RhF_6 , obtained from Density Functional Theory in the Generalized Gradient Approximation²⁴ using the full-potential linear augmented wave formalism as implemented in WIEN2K²⁵, and using the experimental crystal structures.^{26,27} When the SOC is not taken into account, both compounds have very similar DOS (Fig. 2a-b): There is a narrow (~ 400 meV) band that consists of the transition metal t_{2g} states, which is partially occupied. The t_{2g} - e_g splitting is ~ 3 eV, and the e_g states are well above the Fermi level. There is no other state than the t_{2g} states around the Fermi level for a 4-5 eV interval.

The strong spin orbit coupling due to the heavy Ir ion in Rb_2IrF_6 dramatically alters the band structure of this compound (Fig. 2c). The partially filled t_{2g} band near the Fermi level is split into two bands, a lower lying $J_{eff} = 3/2$ band with 4 electrons, and a half filled $J_{eff} = 1/2$ band that crosses the Fermi level. The latter is extremely narrow (~ 100 meV) but since the Mott physics is beyond DFT, this theory predicts metallic state. The Rh ion in Rb_2RhF_6 , which is above Ir in the periodic table, introduces a much weaker SOC than Ir. As a result, even when SOC is taken into account, the $J_{eff} = 3/2$ states are not energetically separated from the $J_{eff} = 1/2$ ones. However, it is still possible to identify the two overlapping peaks corresponding to these two groups of states in the DOS.

Both of these compounds have narrow, half filled $J_{eff} = 1/2$ bands near the Fermi level, indicating that a small amount of on-site correlations can drive them into a Mott-insulating state. While this state is beyond DFT at the GGA level, it is possible to capture the Mott insulating phase using Dynamical Mean Field Theory (DMFT).²⁸ DFT+DMFT has been successfully applied to reproduce the properties of various Mott insulators and it has been recently used to study the $J_{eff} = 1/2$ insulating phase in Sr_2IrO_4 .⁵ As a result, it is the natural method of choice to study the possibly Mott insu-

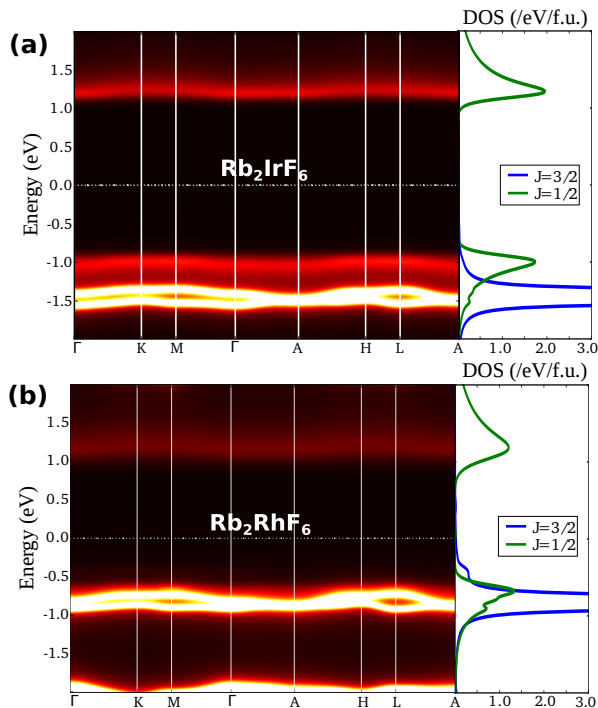


FIG. 3. The spectral function $A(k, \omega)$ and DOS of (a) Rb_2IrF_6 , and (b) Rb_2RhF_6 (bottom).

lating electronic structure of the hexafluoro-iridates and -rhodates. We chose the same on-site Coulomb repulsion in these compounds as estimated for iridates in Ref. 5, i.e., $U = 4.5\text{eV}$ and $J = 0.8\text{eV}$. We note that these values are the lower bound for more localized fluorides, hence we are possibly underestimating the size of the Mott gap.

In Fig. S1, we present the result of our DMFT calculations: The spectral functions $A(k, \omega)$ of Rb_2IrF_6 and Rb_2RhF_6 from DFT+DMFT.²⁹ Both compounds are Mott insulators, with wide gaps close to $\sim 2\text{eV}$. In Rb_2IrF_6 , the upper and lower Hubbard bands are clearly separated and have $J_{\text{eff}} = 1/2$ character, indicating that Rb_2IrF_6 is a $J_{\text{eff}} = 1/2$ Mott insulator. In Rb_2RhF_6 , the lower Hubbard band overlaps with the fully occupied, uncorrelated $J_{\text{eff}} = 3/2$ bands and so cannot be clearly seen in the $A(k, \omega)$ plot. However, the upper Hubbard band has a clear $J_{\text{eff}} = 1/2$ character and therefore this compound is a $J_{\text{eff}} = 1/2$ insulator as well. To the best of our knowledge, this is the first report of a $J_{\text{eff}} = 1/2$ insulator in a compound that does not contain Iridium. Furthermore, both of these compounds have the largest gaps ever reported for a $J_{\text{eff}} = 1/2$ insulator. Both the large gaps, and the possibility of the $J_{\text{eff}} = 1/2$ state in a rhodate compound are thanks to the non-connectivity of the MF_6 octahedra in the KGF structure, and the resulting very narrow $J_{\text{eff}} = 1/2$ bands.

In passing, we note that replacing Ir with Rh in Sr_2IrO_4 leads to a metallic phase both because of the much weaker SOC³⁰ but also possibly because of the

slightly larger electronegativity of the Rh ion. In the KGF fluorides, the charge gap is large, which makes the electronegativity difference negligible, and also the SOC is not necessary for the Mott insulating phase (it is essential only for the $J_{\text{eff}}=1/2$ character). As a result, even the rhodates in this structure are $J_{\text{eff}}=1/2$ Mott insulators. (See the supplemental material.)

Encouraged by the success of our strategy to look for $J_{\text{eff}} = 1/2$ Mott insulators in this class of compounds, we also performed DFT+DMFT calculations in three other compounds with the same crystal structure, Cs_2IrF_6 , K_2IrF_6 , and K_2RhF_6 . While these compounds have significantly different lattice constants due to the different alkali metals they contain, we find all of them to be $J_{\text{eff}} = 1/2$ insulators with large gaps as well. All of these compounds were synthesized and their crystal structures were studied before^{22,23,26,27,31–33} but there is very little information on their magnetic properties or conductivities. Our predictions call for more experiments to characterize these materials better. We predict a fluctuating magnetic moment of $1.6\mu_B$ in both Rb_2IrF_6 and Rb_2RhF_6 , which is smaller than the value expected for an ideal spin-1/2 Mott insulator ($1.73\mu_B$) because of the charge fluctuations (there is a $> 10\%$ probability that there are 6 electrons in the t_{2g} orbitals). These values are $\sim 12\%$ larger than what is measured in Cs_2IrF_6 in Ref. 31, but $\sim 8\%$ smaller than the value measured in the Rh compounds in Ref. 26 at room temperature.

The ideal $J_{\text{eff}} = 1/2$ state is $SU(2)$ invariant, and so it has no magnetic anisotropy. However, systems such as Sr_2IrO_4 are observed not to be exactly at this limit due to deviations of the wave function from the ideal $J_{\text{eff}} = 1/2$.¹⁰ The reason is that Sr_2IrO_4 lacks cubic symmetry: It has the space group $I4_1/acd$, which is tetragonal, and hence the three t_{2g} orbitals of the Ir ion are split into a degenerate doublet and a singlet. The deviation from ideal $J_{\text{eff}} = 1/2$ state is small but not negligible, and it depends strongly on biaxial strain and pressure.^{5,12,34} In the KGF structure, the space group is trigonal, and the t_{2g} irreducible representation is split into two, a singlet A_{1g} and a doublet E_g , similar to Sr_2IrO_4 . This also introduces a deviation from the $J_{\text{eff}} = 1/2$ state and a resultant magnetic anisotropy.

In order to see how much the wavefunction is different from the ideal $J_{\text{eff}} = 1/2$ state, we study the hybridization function $\Delta(\omega)$ used in the DMFT calculation.³⁵ It is given by

$$\frac{1}{\omega - \Delta(\omega) - \Sigma(\omega)} = \sum_{\vec{k}} \hat{P}_{\vec{k}} \frac{1}{\omega + \mu - \epsilon_{\vec{k}} - \hat{P}_{\vec{k}}^{-1} \Sigma(\omega)} \quad (1)$$

where $\Sigma(\omega)$ is the DMFT self energy, $\epsilon_{\vec{k}}$ are the DFT Kohn-Sham eigenvalues, and \hat{P} and \hat{P}^{-1} are the projector and the embedder on the transition metal site. In the high frequency limit $\omega \rightarrow \infty$, the eigenvalues of the Δ matrix give the atomic energy levels (including both the crystal field and the spin-orbit coupling) and it is related to the single ion anisotropy. In the

$\omega \rightarrow 0$ limit, it is related to the low energy electronic excitations. The two eigenvectors of Δ with the largest eigenvalues are the $J_{eff} = 1/2$ -like states $|\psi_{+1/2}\rangle$ and $|\psi_{-1/2}\rangle$. The inner products of these with the ideal $J_{eff} = 1/2$ states $|J_{1/2,\mp 1/2}\rangle$ can be used as a measure of how close the system to the $SU(2)$ limit is. However, this product is second order in the mixing, and a better measure is the coefficients in the expansions of $|\psi_{\mp 1/2}\rangle$.

$$|\psi_{+1/2}\rangle = \frac{\sqrt{3-2\gamma^2}}{3} \left(-|a_1 \downarrow\rangle + (1-i)|a_1 \uparrow\rangle \right) + \frac{\gamma}{3} \left([-|e_+ \downarrow\rangle + (\alpha^2 - i\alpha)|e_+ \uparrow\rangle] + [-|e_- \downarrow\rangle + (\alpha - i\alpha^2)|e_- \uparrow\rangle] \right) \quad (2)$$

$$|\psi_{-1/2}\rangle = \frac{\sqrt{3-2\gamma^2}}{3} \left(-|a_1 \uparrow\rangle + (1+i)|a_1 \downarrow\rangle \right) + \frac{\gamma}{3} \left([|e_+ \uparrow\rangle + (\alpha^2 + i\alpha)|e_+ \downarrow\rangle] + [|e_- \uparrow\rangle + (\alpha + i\alpha^2)|e_- \downarrow\rangle] \right) \quad (3)$$

Here, γ quantifies the deviation from the ideal limit, and $\gamma = 1$ gives $|\psi_{\mp 1/2}\rangle = |J_{1/2,\mp 1/2}\rangle$. A large $|1-\gamma|$ indicates strong deviation from the Heisenberg regime, and leads to large magnon gaps, even larger than the spin wave bandwidth in $\text{Sr}_3\text{Ir}_2\text{O}_7$.^{5,37} Since hybridization is frequency dependent, so is γ . In Rb_2IrF_6 , the low frequency $\gamma_0 = 0.987$ and the high frequency $\gamma_\infty = 0.992$. Compared to Sr_2IrO_4 ,⁵ which has $\gamma_0 = 1.03$ and $\gamma_\infty = 1.02$; the electronic state in Rb_2IrF_6 is much more isotropic, and closer to the ideal $SU(2)$ limit. The rhodate compound Rb_2RhF_6 , which has weaker SOC, shows a more significant deviation from the ideal limit: It has $\gamma_0 = 1.020$ and $\gamma_\infty = 0.935$.

This very isotropic behaviour despite the noncubic spacegroup of Rb_2IrF_6 can be better understood considering the local coordination geometry of the transition metal ion. The site symmetry of Ir is $\bar{3}m$. The elements of the point group include various rotations, such as a threefold rotation around $[001]$ and a twofold rotation around $[100]$ (Fig. 1c). As a result, all six F-ligands around a M ion are symmetry equivalent: They are chemically identical, and their F-M bond lengths are the same. The deviation from the ideal cubic symmetry on the M site is only due to the presence of further neighbours that reduce the symmetry, and the deviation of the F-octahedra from a regular octahedron. This latter effect is quite small (the largest F-M-F bond angle variance in the compounds we consider is less than 6 degrees), and as a result, the Ir ion is in an almost cubic environment. In the RP family of iridate compounds, the site symmetry of the Ir ion can be as high as $4/mmm$. However, despite a 4-fold rotation and various 2-fold rotation axes that pass through the Ir ion (Fig. 1d), there is no 3-fold

This measure is used in Ref. [5] to study the effect of tetragonal symmetry breaking in Sr_2IrO_4 . Under a trigonal perturbation, the t_{2g} orbitals are split into a singlet and a doublet as³⁶ $|a_1\rangle = \frac{1}{\sqrt{3}}(|d_{xy}\rangle + |d_{yz}\rangle + |d_{xz}\rangle)$, $|e_+\rangle = \frac{1}{\sqrt{3}}(|d_{xy}\rangle + \alpha|d_{yz}\rangle + \alpha^2|d_{xz}\rangle)$, and $|e_-\rangle = \frac{1}{\sqrt{3}}(|d_{xy}\rangle + \alpha^2|d_{yz}\rangle + \alpha|d_{xz}\rangle)$, where $\alpha = e^{i2\pi/3}$. A generalization of the $J_{eff} = 1/2$ states that takes into account this splitting is

rotation in the point group, and there are two *chemically* distinct ligands around each Ir ion. The apical oxygens, shown by red in Fig. 1d, are bonded to only one Ir ion, whereas the other oxygens are bonded to two Ir each. This necessarily results in very a noncubic *local* environment of the Ir ion, which leads to deviations from the ideal $J_{eff} = 1/2$ state even when the Ir-O bondlengths are artificially set to be equal.

In conclusion, we identified a new class of $J_{eff} = 1/2$ Mott insulators, which includes the first two examples of such compounds without iridium. These materials are wide gap Mott insulators, with no visible tendency towards magnetic ordering, and some of them are also closer to the isotropic $SU(2)$ limit than the well studied Sr_2IrO_4 . This work extends the search for new materials which display an interplay of correlations with spin-orbit coupling to fluoride compounds. We posit that the $J_{eff} = 1/2$ Mott insulating phase is very common in transition metal fluorides with isolated Ir^{4+}F_6 and Rh^{4+}F_6 complexes. Studying other structure types that satisfy this property would lead not only to the discovery of new $J_{eff} = 1/2$ Mott insulators but also many other strongly correlated complex fluorides with interesting physical properties.

Note: While this manuscript was under review, we became aware of a study on RuCl_3 which also reports a relativistic Mott insulating phase in a 4d transition metal halide.³⁸

We acknowledge fruitful discussions with N.A. Benedek and O. Erten. T. B. was supported by the Rutgers Center for Materials Theory, and K. H. was supported by NSF DMR-1405303 and NSF DMREF-1233349.

¹ W. Witczak-Krempa, G. Chen, Y. B. Kim, and L. Balents, Annual Review of Condensed Matter Physics **5**, 57 (2014).

² X. Wan, A. M. Turner, A. Vishwanath, and S. Y. Savrasov,

- Phys. Rev. B **83**, 205101 (2011).
- ³ S. J. Moon, H. Jin, K. W. Kim, W. S. Choi, Y. S. Lee, J. Yu, G. Cao, A. Sumi, H. Funakubo, C. Bernhard, and T. W. Noh, Phys. Rev. Lett. **101**, 226402 (2008).
 - ⁴ Y. K. Kim, O. Krupin, J. D. Denlinger, A. Bostwick, E. Rotenberg, Q. Zhao, J. F. Mitchell, J. W. Allen, and B. J. Kim, Science (2014), 10.1126/science.1251151.
 - ⁵ H. Zhang, K. Haule, and D. Vanderbilt, Phys. Rev. Lett. **111**, 246402 (2013).
 - ⁶ B. Kim, H. Ohsumi, T. Komesu, S. Sakai, T. Morita, H. Takagi, and T. Arima, Science **323**, 1329 (2009).
 - ⁷ M. A. Laguna-Marco, D. Haskel, N. Souza-Neto, J. C. Lang, V. V. Krishnamurthy, S. Chikara, G. Cao, and M. van Veenendaal, Phys. Rev. Lett. **105**, 216407 (2010).
 - ⁸ W. Ju, G.-Q. Liu, and Z. Yang, Phys. Rev. B **87**, 075112 (2013).
 - ⁹ B. J. Kim, H. Jin, S. J. Moon, J.-Y. Kim, B.-G. Park, C. S. Leem, J. Yu, T. W. Noh, C. Kim, S.-J. Oh, J.-H. Park, V. Durairaj, G. Cao, and E. Rotenberg, Phys. Rev. Lett. **101**, 076402 (2008).
 - ¹⁰ S. Fujiyama, H. Ohsumi, K. Ohashi, D. Hirai, B. J. Kim, T. Arima, M. Takata, and H. Takagi, Phys. Rev. Lett. **112**, 016405 (2014).
 - ¹¹ J. Gunasekera, Y. Chen, J. Kremenak, P. Miceli, and D. Singh, arXiv preprint arXiv:1405.0512 (2014).
 - ¹² D. Haskel, G. Fabbri, M. Zhernenkov, P. P. Kong, C. Q. Jin, G. Cao, and M. van Veenendaal, Phys. Rev. Lett. **109**, 027204 (2012).
 - ¹³ J. S. Lee, Y. Krockenberger, K. S. Takahashi, M. Kawasaki, and Y. Tokura, Phys. Rev. B **85**, 035101 (2012).
 - ¹⁴ C. Liu, S.-Y. Xu, N. Alidoust, T.-R. Chang, H. Lin, C. Dhi-tal, S. Khadka, M. Neupane, I. Belopolski, G. Landolt, *et al.*, arXiv preprint arXiv:1403.2704 (2014).
 - ¹⁵ C. Martins, M. Aichhorn, L. Vaugier, and S. Biermann, Phys. Rev. Lett. **107**, 266404 (2011).
 - ¹⁶ M. M. Sala, K. Ohgushi, A. Al-Zein, Y. Hirata, G. Monaco, and M. Krisch, arXiv preprint arXiv:1402.0893 (2014).
 - ¹⁷ S. Fujiyama, H. Ohsumi, T. Komesu, J. Matsuno, B. J. Kim, M. Takata, T. Arima, and H. Takagi, Phys. Rev. Lett. **108**, 247212 (2012).
 - ¹⁸ R. Arita, J. Kuneš, A. V. Kozhevnikov, A. G. Eguiluz, and M. Imada, Phys. Rev. Lett. **108**, 086403 (2012).
 - ¹⁹ F. Wang and T. Senthil, Phys. Rev. Lett. **106**, 136402 (2011).
 - ²⁰ A. Nozaki, H. Yoshikawa, T. Wada, H. Yamauchi, and S. Tanaka, Phys. Rev. B **43**, 181 (1991).
 - ²¹ A. Wells, *Structural Inorganic Chemistry*, Oxford Classic Texts in the Physical Sciences (OUP Oxford, 2012).
 - ²² D. Babel, *Structural chemistry of octahedral fluorocomplexes of the transition elements* (Springer, 1967).
 - ²³ W. Massa and D. Babel, Chemical Reviews **88**, 275 (1988).
 - ²⁴ J. P. Perdew, K. Burke, and M. Ernzerhof, Phys. Rev. Lett. **77**, 3865 (1996).
 - ²⁵ P. Blaha, S. K., M. G., K. D., and L. J., *WIEN2k: An Augmented Plane Wave Program for Calculating Crystal Properties*, Tech. Rep. (2001).
 - ²⁶ E. Weise and W. Klemm, Zeitschrift fuer anorganische und allgemeine Chemie **272**, 211 (1953).
 - ²⁷ A. I. Smolentsev, A. I. Gubanov, D. Y. Naumov, and A. M. Danilenko, Acta Crystallographica Section E - Structure Reports Online **63**, I200 (2007).
 - ²⁸ In the DFT+DMFT implementation that we used³⁵, a self energy Σ which contains all Feynman diagrams local to the Ir ion is added to the Kohn-Sham Hamiltonian. The self energy is obtained by solving the local impurity problem using continuous time quantum Monte Carlo^{39,40} and full charge self-consistency is obtained by repeating DFT and DMFT steps.
 - ²⁹ In our DMFT calculations, the temperature is taken to be 0.01 eV. While in the beginning of the calculations the symmetry of the self energy is broken and magnetic ordering is allowed, it became spin-symmetric after a few iterations, indicating that the compounds do not have any strong tendency towards magnetic ordering at this temperature.
 - ³⁰ T. F. Qi, O. B. Korneta, L. Li, K. Butrouna, V. S. Cao, X. Wan, P. Schlottmann, R. K. Kaul, and G. Cao, Phys. Rev. B **86**, 125105 (2012).
 - ³¹ M. Hepworth, P. Robinson, and G. Westland, Journal of the Chemical Society (Resumed), 611 (1958).
 - ³² H. Fitz, B. Muller, O. Graudejus, and N. Bartlett, ZEITSCHRIFT FUR ANORGANISCHE UND ALLGEMEINE CHEMIE **628**, 133 (2002).
 - ³³ A. I. Smolentsev, A. I. Gubanov, D. Y. Naumov, and A. M. Danilenko, ACTA CRYSTALLOGRAPHICA SECTION E-STRUCTURE REPORTS ONLINE **63**, I201 (2007).
 - ³⁴ C. R. Serrao, J. Liu, J. Heron, G. Singh-Bhalla, A. Yadav, S. Suresha, R. Paull, D. Yi, J.-H. Chu, M. Trassin, *et al.*, Physical Review B **87**, 085121 (2013).
 - ³⁵ K. Haule, C.-H. Yee, and K. Kim, Phys. Rev. B **81**, 195107 (2010).
 - ³⁶ B.-J. Yang and Y. B. Kim, Phys. Rev. B **82**, 085111 (2010).
 - ³⁷ J. Kim, A. H. Said, D. Casa, M. H. Upton, T. Gog, M. Daghofer, G. Jackeli, J. van den Brink, G. Khaliullin, and B. J. Kim, Phys. Rev. Lett. **109**, 157402 (2012).
 - ³⁸ K. W. Plumb, J. P. Clancy, L. J. Sandilands, V. V. Shankar, Y. F. Hu, K. S. Burch, H.-Y. Kee, and Y.-J. Kim, Phys. Rev. B **90**, 041112 (2014).
 - ³⁹ K. Haule, Phys. Rev. B **75**, 155113 (2007).
 - ⁴⁰ E. Gull, A. J. Millis, A. I. Lichtenstein, A. N. Rubtsov, M. Troyer, and P. Werner, Rev. Mod. Phys. **83**, 349 (2011).
 - ⁴¹ K. Haule, T. Birol, and G. Kotliar, Phys. Rev. B **90**, 075136 (2014).

Supplemental Information for
“The $J_{eff} = 1/2$ Mott Insulating State in Rh and Ir Fluorides”

I. DETAILS OF THE DMFT IMPLEMENTATION

The action of the auxiliary impurity problem that we minimize in our calculations is

$$\begin{aligned} \mathcal{S} = & \int_0^\beta d\tau \psi_{L\sigma}^\dagger(\tau) \frac{\partial}{\partial \tau} \psi_{L\sigma}(\tau) + \int_0^\beta d\tau \int_0^\beta d\tau' \psi^\dagger(\tau') \Delta_{L_1\sigma, L_2\sigma'} \psi(\tau) \\ & + \frac{1}{2} \int_0^\beta d\tau \sum_{L_1, L_2, L_3, L_4, \sigma, \sigma'} U_{L_1, L_2, L_3, L_4} \psi_{L_1\sigma}^\dagger(\tau) \psi_{L_2\sigma'}^\dagger(\tau) \psi_{L_3\sigma'}(\tau) \psi_{L_4\sigma}(\tau) \end{aligned} \quad (\text{S1})$$

where τ is the imaginary time, ψ is the annihilation operator for the impurity electrons, L and σ are the orbital and spin indices, and Δ is the impurity hybridization function. The on site electron-electron Coulomb interaction between the d electrons is represented by the Slater form:

$$\hat{U} = \frac{1}{2} \sum_{L_1, L_2, L_3, L_4, \sigma, \sigma'} U_{L_1, L_2, L_3, L_4} c_{L_1\sigma}^\dagger c_{L_2\sigma'}^\dagger c_{L_3\sigma'} c_{L_4\sigma} \quad (\text{S2})$$

and

$$U_{L_1, L_2, L_3, L_4} = \sum_k \frac{4\pi}{2k+1} \langle Y_{L_1} | Y_{km} | Y_{L_4} \rangle \langle Y_{L_2} | Y_{km}^* | Y_{L_3} \rangle F_{l_1, l_2, l_3, l_4}^k \quad (\text{S3})$$

Here, Y are the radial part of the spherical harmonics, the index L denotes $L \rightarrow \{l, m\}$, and F^k are the Slater integrals. The explicit form of the frequency dependent hybridization $\Delta(i\omega)$ can be written in terms of the projector P , the Kohn-Sham Hamiltonian (without the spin-orbit coupling) \mathcal{H}^{DFT} , the spin-orbit coupling Hamiltonian \mathcal{H}^{SOC} , the self-energy $\Sigma(i\omega)$, the local Green's function $G_{loc}(i\omega)$ and the double counting energy V_{DC} as^{S1}

$$\Delta_{L\sigma, L'\sigma'}(i\omega) = \sum_{\vec{k}, i, j} P_{\vec{k}}(L\sigma, L'\sigma', ij) (\mathcal{H}^{DFT} + \mathcal{H}^{SOC}) + i\omega - \Sigma(i\omega) - G_{loc}^{-1}(i\omega) - V_{dc} \quad (\text{S4})$$

The small latin indices i, j enumerate the Kohn-Sham bands and include the spin as well. \vec{k} is the crystal momentum. The form of the spin-orbit coupling Hamiltonian is $\mathcal{H}^{SOC} \sim \lambda \vec{L} \cdot \vec{S}$. Forms of different projectors (P) and double counting (V_{DC}) have been previously discussed in, for example, [S1] and [S2]. Σ , G_{loc} , \mathcal{H}^{DFT} , and \mathcal{H}^{SOC} are determined self consistently by extremizing the action (S1), hence Σ and G_{loc} obey the DMFT self consistency condition and \mathcal{H}^{DFT} , and \mathcal{H}^{SOC} are determined from the self consistent electronic charge.

The impurity model is solved with the continuous time quantum monte carlo (CTQMC) solver. In order to reduce the sign problem, we employ orbital and spin rotations (\mathcal{U}) that cast the hybridization Δ in a diagonal form in the relevant low energy limit

$$\Delta(i\omega) = \mathcal{U}^\dagger \Delta_{diag}(i\omega) \mathcal{U} + \delta\Delta(i\omega) \quad (\text{S5})$$

The hybridization is strongly frequency dependent, however, its eigenvectors do not change much with frequency. In other words, it is possible to obtain an *almost diagonal hybridization* by using a *frequency independent* rotation \mathcal{U} . We ignore the off diagonal $\delta\Delta(i\omega)$ and as a result our CTQMC impurity solver suffers very little sign problem, even in the presence of spin-orbit coupling and low crystal symmetry.

II. THE EFFECT OF SPIN-ORBIT COUPLING ON THE INSULATING BEHAVIOUR

Unlike Sr_2IrO_4 , where spin-orbit coupling (SOC) is necessary for the insulating behaviour, the compounds with the KGF structure that we consider can be Mott insulators even in the absence of SOC, because they have narrow bands in DFT even without SOC. In order to verify this point, we performed DFT+DMFT calculations without SOC on Rb_2RhF_6 and Rb_2IrF_6 . The DOS from these calculations, along with the DOS with SOC for comparison, are presented in Figure 1. As expected from a crystal structure with unconnected polyhedra, both of these compounds

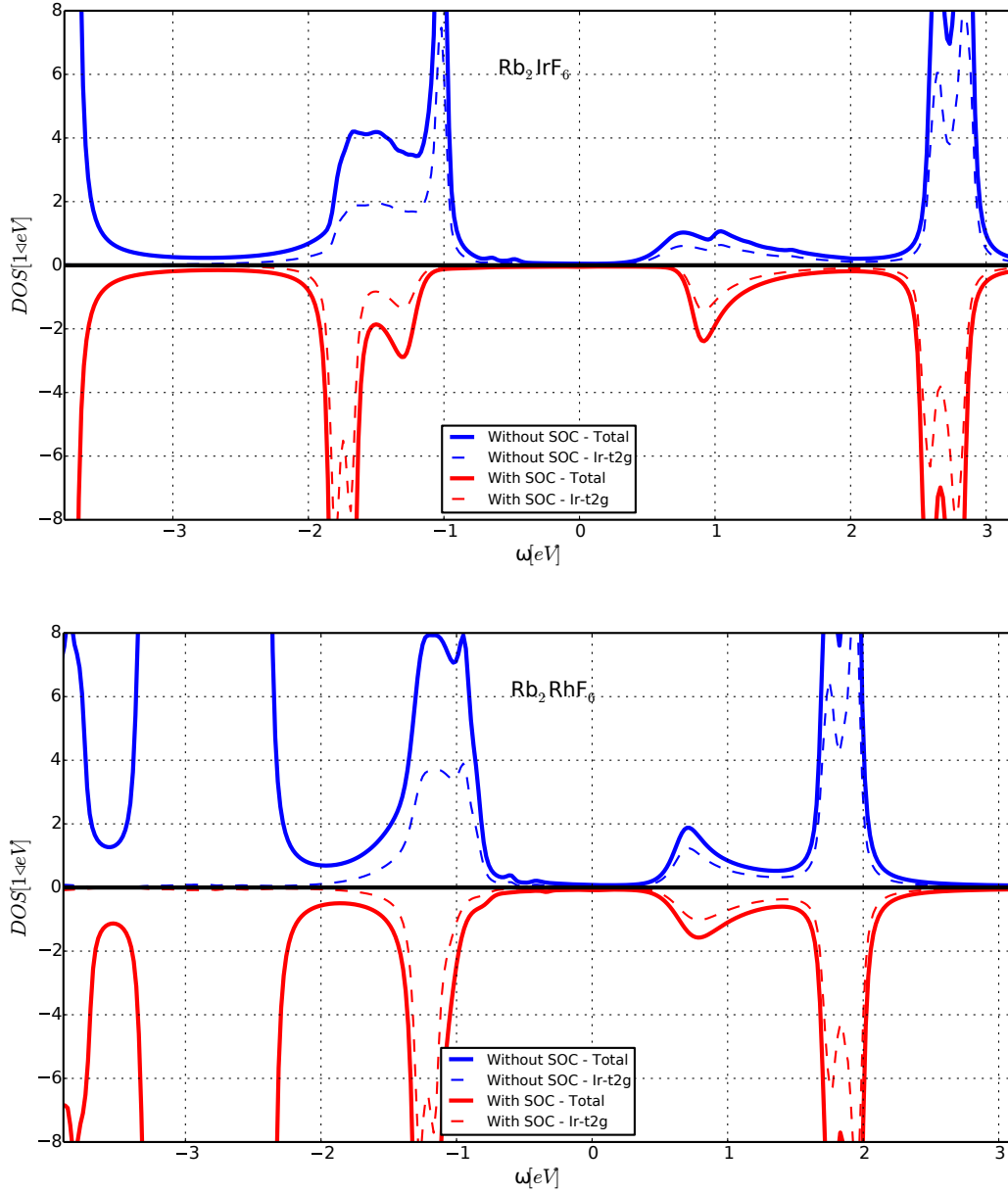


FIG. S1. The densities of states for Rb_2IrF_6 and Rb_2RhF_6 with and without spin orbit coupling.

are Mott insulators with wide charge gaps. Rb_2IrF_6 has a smaller gap when SOC is not taken into account, but the width of the gap of Rb_2RhF_6 does not change much, in line with the small energy scale of the SOC in this compound.

As a result, we conclude that the SOC in the TM-fluorides with the KGF structure is not responsible of the insulating behaviour, but it only changes the character of the insulating state. In the absence of SOC, these compounds would be spin-1/2 Mott insulators, whereas, due to SOC, they become $J_{eff}=1/2$ Mott insulators. This difference is clear considering the character of the low energy degrees of freedom, and would be visible in magnetic properties, such as the strength of the magnetocrystalline anisotropy or the magnon dispersion.

III. MAGNETIC MOMENTS' DEPENDENCE ON γ AND THE DEVIATION FROM HEISENBERG BEHAVIOUR

In the main text, we generalized the $|J_{1/2, \mp 1/2}\rangle$ states as

$$|\psi_{+1/2}\rangle = \frac{\sqrt{3-2\gamma^2}}{3} \left(-|a_1 \downarrow\rangle + (1-i)|a_1 \uparrow\rangle \right) + \frac{\gamma}{3} \left([-|e_+ \downarrow\rangle + (\alpha^2 - i\alpha)|e_+ \uparrow\rangle] + [-|e_- \downarrow\rangle + (\alpha - i\alpha^2)|e_- \uparrow\rangle] \right) \quad (S6)$$

$$|\psi_{-1/2}\rangle = \frac{\sqrt{3-2\gamma^2}}{3} \left(-|a_1 \uparrow\rangle + (1+i)|a_1 \downarrow\rangle \right) + \frac{\gamma}{3} \left([|e_+ \uparrow\rangle + (\alpha^2 + i\alpha)|e_+ \downarrow\rangle] + [|e_- \uparrow\rangle + (\alpha + i\alpha^2)|e_- \downarrow\rangle] \right) \quad (S7)$$

where

$$|a_1\rangle = \frac{1}{\sqrt{3}} (|d_{xy}\rangle + |d_{yz}\rangle + |d_{xz}\rangle) \quad (S8)$$

$$|e_+\rangle = \frac{1}{\sqrt{3}} (|d_{xy}\rangle + \alpha|d_{yz}\rangle + \alpha^2|d_{xz}\rangle) \quad (S9)$$

$$|e_-\rangle = \frac{1}{\sqrt{3}} (|d_{xy}\rangle + \alpha^2|d_{yz}\rangle + \alpha|d_{xz}\rangle) \quad (S10)$$

and $\alpha = e^{i2\pi/3}$. These states are the eigenstates of the SOC Hamiltonian under a trigonal distortion, which breaks the degeneracy of $|a_1\rangle$ with $|e_{\mp}\rangle$. The ideal $J_{eff}=1/2$ states $|J_{1/2, \mp 1/2}\rangle$ are SU(2) invariant: the ratio of orbital to spin angular momenta is $\langle\mu_L\rangle/\langle\mu_S\rangle = 2$ and is independent of direction. However, the generalized states $|\psi_{\mp 1/2}\rangle$ do not satisfy these conditions. For example, for z being the axis of trigonal distortion, and $x = \gamma - 1 \ll 1$, one gets $\langle\mu_L^z\rangle/\langle\mu_S^z\rangle = 2 - 2x^2$. In this respect, γ is a natural parameter to quantify the deviation of the system from an ideal $J_{eff}=1/2$ insulator.

The fact that the magnetic moment is anisotropic, and that the system is not in a Heisenberg regime, has important consequences in the magnetic excitation spectrum. For example, $\text{Sr}_3\text{Ir}_2\text{O}_7$, which has a $|1-\gamma|$ that is much larger than Sr_2IrO_4 , has a large (92 meV) magnon gap that is even wider than the magnon bandwidth in this compound.^{S3,S4}

[S1] K. Haule, C.-H. Yee, and K. Kim, Phys. Rev. B **81**, 195107 (2010).

[S2] K. Haule, T. Birol, and G. Kotliar, Phys. Rev. B **90**, 075136 (2014).

[S3] H. Zhang, K. Haule, and D. Vanderbilt, Phys. Rev. Lett. **111**, 246402 (2013).

[S4] J. Kim, A. H. Said, D. Casa, M. H. Upton, T. Gog, M. Daghofer, G. Jackeli, J. van den Brink, G. Khaliullin, and B. J. Kim, Phys. Rev. Lett. **109**, 157402 (2012).